analytical chemistry

ARTICLE

pubs.acs.org/ac

Combining Surface Plasmon Resonance (SPR) Spectroscopy with Surface-Enhanced Raman Scattering (SERS)

Stefan A. Meyer, Eric C. Le Ru, and Pablo G. Etchegoin*

The MacDiarmid Institute for Advanced Materials and Nanotechnology, School of Chemical and Physical Sciences, Victoria University of Wellington, P.O. Box 600, Wellington, New Zealand.

Supporting Information

ABSTRACT: The simultaneous measurement of surface plasmon resonance (SPR) spectroscopy and surface-enhanced Raman scattering (SERS) on flat metallic surfaces is demonstrated on a relatively simple experimental setup based on the Kretschmann configuration. This setup requires only minor modifications to standard Raman microscopes, and we show that it can be applied successfully to the most common conditions of SPR spectroscopy, i.e., water-based solutions on gold films. Our results emphasize the peculiar properties of the Kretschmann configuration for spectroscopy in general and SERS measurements in particular, especially in terms of the asymmetry between excitation and collection requirements. The combination of simultaneous SPR−SERS spectroscopy opens up interesting prospects in analytical science to study, for example, reaction kinetics at surfaces under conditions which are already available in commercial SPR instruments.

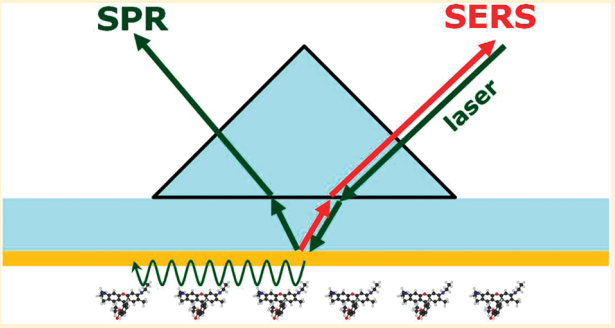

Motivation. From the early days of the technique,[1−3] analytical work has always been hampered in surface-enhanced Raman scattering (SERS)[4,5] by the irreproducibility of the substrates responsible for the Raman enhancement.[6] Accordingly, with the advent of better techniques and more sophisticated control of nanostructures in the past decade,[2,7−9] a great amount of effort has been invested in SERS toward reversing this tendency (while having always fluorescence spectroscopy as the "standard" reference to be surpassed[10]). In this manner, a substantial amount of progress has been achieved in analytical applications of SERS, and it mostly arose through different strategies of tailor-made probes, carefully controlled (nanostructured) substrates and particles, or combinations thereof.[2,7,8,11−15]

Despite these advances, the simplest, most controllable, and best understood plasmonic system undoubtedly remains the flat metallic surface. Unfortunately, flat surfaces are also known to be poor SERS substrates in the absence of roughness, providing virtually no electromagnetic SERS enhancement. This can be partly compensated when propagating surface-plasmon-polaritons (SPPs) are excited at a metal/dielectric interface. In this case, modest, but arguably very useful, SERS enhancement factors (EFs) are predicted.[4] Coupling to SPPs on planar substrates is routinely done in the well established (and commercially available) technique of surface plasmon resonance (SPR) spectroscopy (with a long history in biomolecular spectroscopy[17−21]). Excitation through a prism is required in SPR spectroscopy for SPP excitation,[4,22,23] with the most common setups being the so-called Otto[24] and Kretschmann[25] configurations. The latter, as depicted schematically in Figure 1 and further explained in the text later, is in fact by far the most commonly used configuration in commercial applications of the technique.

In this paper, we shall aim at demonstrating a combined SPR−SERS study that profits from both techniques simultaneously. From the point of view of SERS, a simple and efficient setup in the Kretschmann configuration opens up the possibility of performing SERS with uniform (and predictable) enhancements on flat planar metallic films. Some of the advantages are obvious: (i) an unsurpassed control over the SERS enhancement factor (EF) distribution (since it is perfectly uniform in the absence of roughness); and (ii) the possibility of accurate and relatively easy theoretical predictions (not subject to uncertainties in the geometry). Such advantages are invaluable for fundamental studies of the SERS effect. For example, the study of molecular orientation effects, i.e., surface selection rules,[26,27] or studies of the "chemical enhancement" (since the electromagnetic enhancement is then well known). But besides the fundamental aspects, there is an even greater attraction to expand the capabilities of SPR spectroscopy with additional information provided by SERS. Simultaneous SPR−SERS spectroscopy could potentially open up new horizons in the understanding of reaction kinetics at surfaces and other important topics in analytical and bioanalytical sciences.

Previous Work. A short historical background is necessary here to put the new aspects in perspective. By itself, SERS in the Kretschmann configuration (KC) is by no means a new idea. It

Received: December 15, 2010
Accepted: January 17, 2011
Published: February 15, 2011

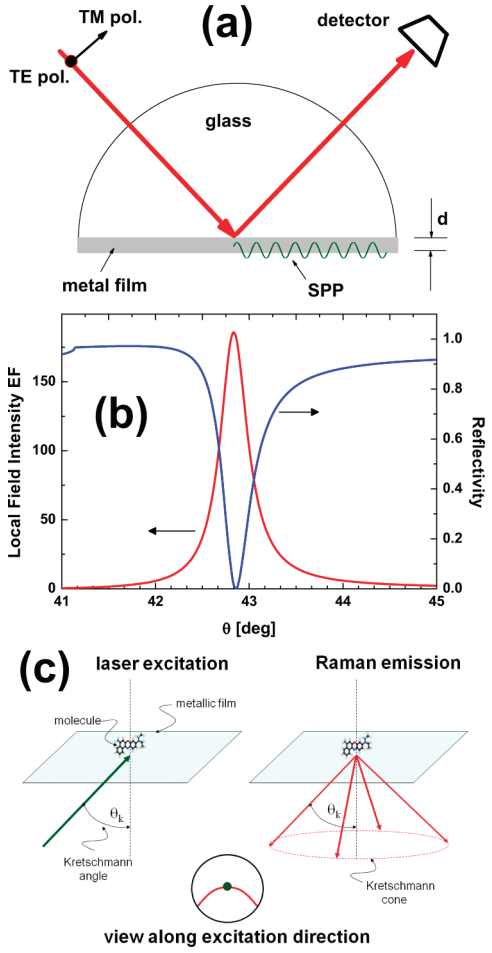

Figure 1. (a) Schematics of the Kretschmann configuration,[16] which couples a light beam (red) incident from a higher n medium (the prism), to the surface-plasmon-polariton (SPP) excitation at a metal/air interface on the other side, by going through a metal film (~20−50 nm). Only TM-polarized light couples to SPPs. Depending on the wavelength, there will be a well-defined optimum angle of incidence where the coupling of the beam with the SPPs is maximized. This is normally observed in surface plasmon resonance (SPR) spectroscopy as a sharp "dip" in reflectivity as shown in part b for a 50 nm Ag film (calculated using the tools of Appendix F in ref 4), and is associated with a large local field intensity enhancement factor (LFIEF) at the surface (shown also in part b). The SERS process in this configuration is depicted schematically in part c. At the resonance, the molecules are excited at the Kretschmann angle θ_K (with TM-polarization) and the Raman-shifted light is emitted at a very similar angle, but in any direction, i.e., in the Kretschmann cone. If we collect light in backscattering through a circle of fixed size (defined by the numerical aperture (NA) of the collecting optics), we see that the fraction of the collected Kretschmann cone depends linearly on the NA. Part of the challenge of combining SPR with SERS is in the simultaneous optimization of both the excitation of SPPs and the collection of the Kretschmann cone.

had been predicted theoretically[28] even before the discovery of the SERS effect and was investigated experimentally on-and-off from the early days. These early experiments, however, were carried out on rough silver films.[29−31] In fact, no SERS signal could be observed in them before the metallic film was electrochemically roughened.[29,31] It is very well-known that roughness is an important factor contributing to SERS,[1] and that rough metallic films are simple SERS substrates with reasonable average EFs. Roughness, however, defeats the purpose of uniform and controllable enhancements that flat surfaces promise, and also prevents (to some degree) the combination of the technique with SPR spectroscopy (by making the resonance condition broader and therefore less sensitive). Following these very early studies, SERS in the KC was carefully and much more convincingly studied (both experimentally and theoretically) in a series of papers in the 1980s,[32−35] again on Ag films. Giergel et al., for example, provide a detailed summary of the findings up to 1988 in ref 35. The additional benefit of collecting the light on the prism side and observing the peculiar emission pattern in the form of a Kretschmann cone (see Figure 1)[33] was clearly identified. SERS signals from both liquids[32−34] and adsorbates[33,35] were successfully measured, and their expected angular dependences (in the form of SPP resonances in incident or scattered light) were observed. Although care was taken in fabricating smooth silver films, the absence of contributions of any roughness to SERS was not demonstrated. Also, in all these cases, relatively complex optical setups were used (with independent excitation and collection) and the overall throughput of the system was not optimized (in some cases, no lens were used to collect the Raman signal).

Following further the historical line, most reports of SERS in the KC in the 1990s focused on a new technical development of the technique to allow the collection of the whole Kretschmann cone on the prism side, using either mirrors[36] or the so-called Weierstrass prism.[37−40] Some of these studies, in fact, used the Otto configuration.[38−40] The improvements in terms of collection efficiency come here at the cost of increased complexity in the optical setup, making these approaches incompatible with standard SPR spectroscopy configurations.

Over the past decades, reports of SERS in the KC have not focused on the understanding of the method, but mostly on its practical use as a characterization tool.[41,42] We also note a recent report[43] of SERS in the KC where light is collected on the air side (despite the fact that the prism side is predicted theoretically to be a better option) and where a SERS EF of over ~10^6 is reported. Such a large EF is impossible to justify theoretically and can only be explained by a large roughness contribution.

This brief review of the existing work on SERS in the KC highlights a number of outstanding issues in its potential connection with SPR spectroscopy: (1) Can we demonstrate a simple optical layout for SERS in the KC, which would be readily adaptable to SPR spectroscopy? (2) Since all the cited studies but two[40,42] were carried out on silver films (where roughness is in many cases likely to be present and enhance the SERS signals), can this method be convincingly extended to Au films? The latter are, in fact, a better alternative for applications since they can be reliably fabricated with minimal roughness, and are already extensively used in (commercial) SPR spectroscopy instruments.

We therefore propose in what follows to revisit the problem of SERS in the Kretschmann configuration with a view to address these outstanding issues in its connection with SPR. We shall show that under the right conditions the Kretschmann configuration offers a valid alternative for a reliable and homogeneous SERS enhancement that can be combined with SPR spectroscopy simultaneously. We will show that such measurements can, moreover, be reliably understood within standard EM theory with a minimum number of parameters: a tremendous advantage over most SERS systems. We shall also introduce a simple method to measure SERS in backscattering in the Kretschmann configuration using back focal plane illumination to improve

coupling to the resonance and combine a high angular resolution with a good collection efficiency. Our method requires then minimal changes to standard Raman systems to adapt them to the simultaneous use of SERS and SPR. We believe that the combination of the two techniques, with the predicting power displayed in the following sections, can make substantial progress in analytical applications where quantification and detailed understanding is essential.

METHODS AND THEORETICAL RESULTS

For all experimental results, we have used Nile blue (NB) as a model SERS analyte since it has a large (resonant) Raman cross-section at the exciting wavelengths used here (633 and 647 nm) and can be deposited easily on metal surfaces at monolayer or submonolayer coverage by dipping/rinsing techniques (details are provided in the Supporting Information).

Our main aim here is to emphasize the experimental results. However, we shall also present throughout the study several theoretical predictions using standard codes[44] for planar multilayer calculations (based on Appendix F in ref 4). The emission part of the SERS enhancement factors were derived using the optical reciprocity theorem.[4,45] For simple reasons of space, full details on the theoretical aspects will be published elsewhere. All the theoretical results are therefore taken here as *bona fide* comparisons with the predictions of standard electromagnetic theory. However, we only mention here that in order to obtain satisfactory agreement between theory and experiments several factors need to be explicitly included in the calculations. Among them are the following: (i) the presence of the coupling prism (and possibly the film glass slide if the prism is not glass), and how it affects in particular the optical paths of incident and emitted light; (ii) the finite size (waist) of the incoming beam (which is assumed Gaussian); (iii) the explicit presence of all layers (such as the 2 nm titanium adhesion layer for the 50 nm gold films); (iv) the focal length and numerical aperture of the exciting/collecting optics (which affect the spread of incident angles and the range of collected angles); (v) the frequency difference between excitation (laser) and the Stokes-shifted emission (which slightly modifies the resonance angles); (vi) the fact that the NB molecules are adsorbed flat on the metal surface and that their resonant Raman tensors are therefore in-plane (this fact actually reduces substantially the expected SERS intensity, but signal intensity was not an issue in these experiments). With all these ingredients taken into account, we find an outstanding agreement between theory and experiment with, essentially, no fitting parameters. For that reason, and although the emphasis is on the experimental results, we will present in the following the theoretical predictions on the same graphs to convey the point about the predicting power of the SERS–SPR combination. Note that all angle-dependence data are presented as a function of incident internal angle (i.e., the angle inside the glass slide onto which the metal film is deposited); see the Supporting Information for an explanation on how the internal angle inside the prism is connected to the external prism rotation.

SERS IN THE KRETSCHMANN CONFIGURATION IN BACKSCATTERING

The coupling to SPPs on planar surfaces in the Kretschmann configuration is a fundamental (and basic) problem in plasmonics that is treated in details in textbooks.[4,22,23] The sharp resonance in reflectivity, and its high sensitivity to the presence of surface adsorbate, is what is routinely used as an operating principle in SPR spectroscopy.[17−21] A brief introduction is given in the caption of Figure 1, but we focus here on some of the subtler aspects that are relevant to the problem of performing backscattering spectroscopy, SERS in particular, in this configuration.

For SERS we have to contemplate the double situation of coupling to SPPs to deliver the laser to the molecules on the surface (at the so-called Kretschmann angle θ_K), and collect the Raman emitted radiation from them (which is emitted in the so-called Kretschmann cone). This is depicted in Figure 1c. Because the resonant coupling to SPPs is relatively sharp in incident angle (fwhm $\sim 0.5°$) but broad in the spectral (photon energy) domain, the emission at the Raman-shifted frequency occurs over a narrow cone around θ_K. In principle, θ_K for emission is different from that of the incident coupling because of the different wavelength introduced by the Stokes shift.[32] This may be an issue in some cases (and it is explicitly taken into account in the theoretical predictions), but in a first approximation to the problem the change in angle may be neglected, especially for relatively small Raman shifts. However, there is a strong asymmetry between excitation (along a fixed direction) and emission (axial-symmetric, but along the same fixed angle as the incident direction, see Figure 1c). This asymmetry between the geometrical aspects of excitation and emission poses several practical problems, as we shall see in the next subsections.

In order to highlight the details of carrying out spectroscopy in the Kretschmann configuration, we show in Figures 2 and 3 the combined angle-dependent reflectivity and SERS measurements in a simple backscattering configuration. In Figure 3, we show in particular the effect of a focusing lens on the coupling to the SPP resonance.

SERS Angular Resonance with No Collection Lens. The setup with "no lens" in Figure 2a would be the most direct simplification of the setup used in early studies.[32−35] A well collimated beam is required to maximize coupling into the very sharp (in angle) SPP resonance, and therefore, we initially use the laser beam as it is (with no focusing lens). Because of our choice of using the backscattering configuration, no lens can then be used for collection if we do not want to change the divergence of the exciting beam. The SPR signal (reflectivity) of the film can be simultaneously monitored by a simple photodiode detector which is attached to the rotating stage containing the prism and the film. The reflectivity curve, for the situation where we have no lens, is shown in Figure 3d. Concurrently, Figure 2b shows the SERS signal (590 cm^{-1} Raman mode) of a monolayer of Nile blue (NB) in air on Ag (50 nm film) at 647 nm excitation through a glass prism (index of refraction $n = 1.5$) as a function of the internal incident angle θ. As expected, this signal only exists for TM polarization. As can be appreciated from Figure 2b, the SERS signal can be followed through the angular resonance. It goes from being invisible, when the laser is not properly coupled, to being an intense peak well above the noise level with a fwhm of ∼0.5° (comparable to the the fwhm observed in reflectivity in Figure 3d for the "no lens" case). The results in Figure 2b are complemented by those in Figure 2c, where the SERS signal in a much wider frequency range is shown for optimum excitation at the Kretschmann angle. This latter result demonstrates the point we raised before: the resonance is sharp in incident angle but broad in the spectral domain (to allow us, for example, to see simultaneously the 590 and ∼1650 cm^{-1} Raman modes of NB).

Actually it is quite remarkable that the Raman signal from a monolayer of dye can be collected without a lens at all. Excluding

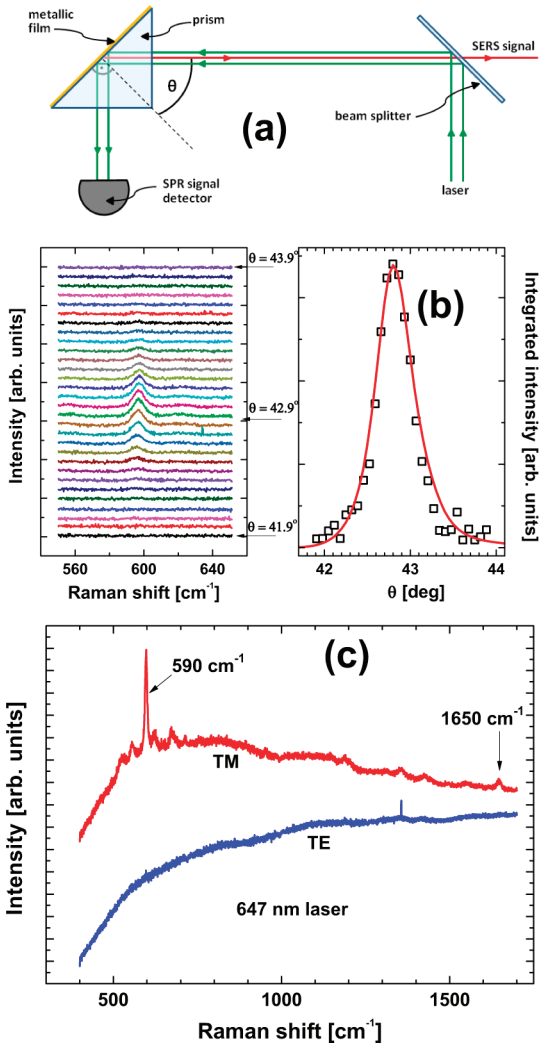

Figure 2. (a) Schematics of the optical setup for combined SPR−SERS in backscattering configuration with no focusing/collecting lens. (b) Experimental angle-dependent SERS signal (symbols) for the 590 cm^{-1} mode of NB deposited on a Ag/air interface (50 nm Ag film) at 647 nm laser excitation (integration time = 18 s, laser power 5 mW). The theoretical prediction is shown as a solid line. The angle of incidence (θ) refers to internal angles inside the glass slide supporting the film (see Supporting Information). (c) Full spectrum of NB at the optimum Kretschmann angle of the 590 cm^{-1} peak for TM and TE polarizations. The Raman peaks are observed only for TM polarization, as expected. The 1650 cm^{-1} mode of NB is visible, albeit with a smaller SERS enhancement factor, thanks to the SPP resonance being relatively broad in wavelength.

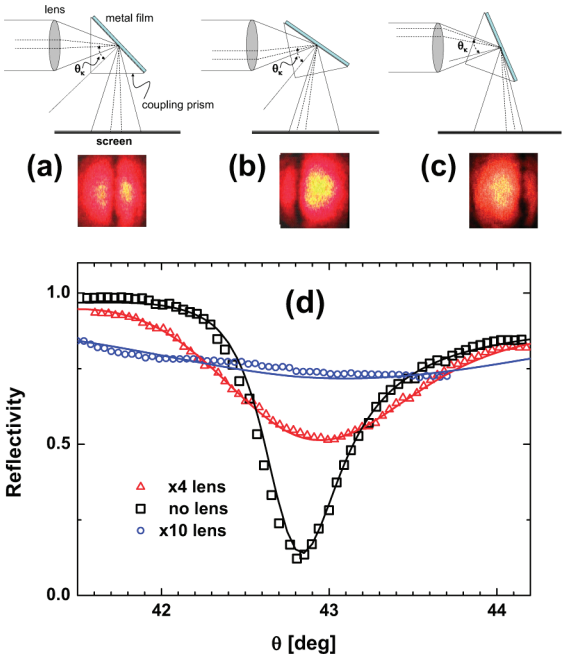

Figure 3. Influence of a focusing lens on the angle-dependent reflectivity. In part d, experimental data (symbols) clearly show the decreased coupling efficiency and broadening as the focal length f of the lens (and indirectly the numerical aperture, NA) increases from the "no lens" case, to a ×4 objective (f = 45 mm, NA = 0.1) and to a ×10 (f = 18 mm, NA = 0.25). The theoretical values (solid lines) are obtained by considering a collimated Gaussian beam of 0.72 mm waist incident on the lenses, therefore resulting in a spread of incident angles at the focal point. The theoretical resonances for plane waves are hence broadened by a convolution of incoming angles produced by the NA of the lens. This effect can be further visualized with the ×10 objective by projecting the image reflected from the sample onto a screen in the far-field, as shown in parts a−c for 3 angle positions. At resonance, a clear black fringe is visible (corresponding to full coupling into the SPP resonance) in the middle of the beam image. However, it is clear that the angular spread of the beam is much larger than that of the resonance resulting in a partial coupling only. This is simultaneously revealed in the corresponding almost flat reflectivity curve in part d.

any roughness contribution to SERS is however difficult with silver films because of their intrinsically low chemical stability. The agreement between theory and experiment in Figures 2 and 3 indicates that roughness is not significant: it would otherwise be revealed in a broadening of the resonance. But this in itself is not clear proof that roughness does not contribute to SERS. Only experiments on gold, where the absence of roughness can be assured more convincingly, will demonstrate unambiguously (as shown later) the ability to carry out SPR−SERS measurement on strictly flat surfaces. However, in order to be able to measure the much weaker SERS signals on gold films, it is first necessary to optimize our collection efficiency. In fact, a large part of the Raman emission is being lost by the restriction that we are collecting only what comes strictly in the backscattering direction. This is a unique situation where the optical requirements to deliver the laser (i.e., a parallel beam) are incompatible with the optical requirements to collect most of the signal in the backscattering configuration. In the case of Figure 2, the effective numerical aperture (NA) for the collection process (without a lens) is really small, and only defined by a narrow acceptance angle related to the paraxial tolerance around the exact optical axis of the spectrometer (we estimate the NA to be ∼0.2 for our system). This was already partially explained (schematically) in Figure 1c. The only reason why a signal can be observed without a lens is because the whole Raman signal is "funneled" into the narrow Kretschmann cone, and we collect here a small fraction of it. We can view the film as behaving as a "1D lens", a unique feature of a sharp angular resonance in emission.

Angular Resonance with a Lens or Microscope Objective. We could of course hope to detect a much larger signal by collecting a larger portion of the Kretschmann cone with a larger NA lens. We can for example use the same setup as in Figure 2a, but with a long working distance microscope objective (to allow

for space for the prism). However, the improvement in collection efficiency has the price of losing the exciting beam collimation (which is now focused by the objective). This results in a decreased coupling into the SPP resonance and a broadening of the angle-dependent reflectivity, which effectively prevents any simultaneous SPR spectroscopy studies. This is illustrated in Figure 3 for two different objectives: ×4 and ×10. It is clear that in the exciting beam produced with, for example, the ×10 objective, only a fraction of the incident rays contained in the converging beam are at the right angle θ_K to couple to the Kretschmann resonance. This is revealed in Figure 3a−c as a "dark fringe" in the far field of the reflected beam (which disappears, as expected, when changing from TM to TE polarization). This dark fringe can easily be followed when rotating the sample, and it gives a good idea of the "angular sharpness" of the resonance and of the angular spread of the exciting beam. If the angle of incidence is changed slightly (by a few degrees), the resonance fringe can be moved to one or the other side of the reflected spot in the far-field, as seen in Figure 3a,c. This is because different fractions of the angular spread of the incoming beam satisfy the resonance condition. This highlights one important aspect: simply using a lens for simultaneous excitation and collection will not be optimal, because only a small fraction of the incident power (only that at the right angle in the beam) couples into the resonance. This is shown more quantitatively in Figure 3d through the reflectivity. It is clear that the use of lenses, even with a small magnification, results in a strong decrease in coupling into the resonance and a concomitant larger broadening. This observation is predicted by theory when taking into account the finite width of the laser beam which is being focused by the lens. The natural (intrinsic) width of the resonance can therefore only be obtained with a collimated beam of small divergence.

Henceforth, these results highlight one of the basic conundrums of the use of the Kretschmann configuration for SERS. Unlike SPR-spectroscopy, that only monitors the reflectivity, we need to take into account in SERS both the delivery of the laser and the collection of the Raman emitted light. If we want to monitor the SERS signal in the backscattering configuration (a very convenient experimental choice), we would benefit from collecting at least part of the Kretschmann cone with a lens of high numerical aperture. However the presence of the lens is incompatible with a simultaneous measurement of SPR, for it prevents optimum coupling to deliver the laser. In the following, we will present a simple modification that enables us to overcome this problem with minimal efforts. We will also illustrate its power by demonstrating simultaneous measurement of SPR reflectivity and SERS on the more difficult system (because of the weaker SERS signals) of Au/air and Au/water interfaces.

■ SPR−SERS MEASUREMENTS ON GOLD FILMS

Principles. It is worth noting that, by using a much more complicated optical setup, with special prisms and/or optics (like the Weierstrass prism[37−40]), one can devise ways to collect the entire Kretschmann cone.[36,37] This was certainly an important improvement in the historical development of both the Kretschmann and Otto configurations. But it comes at the expense of complexity with a customized optical setup with independent excitation and collection directions. In fact, this is the main reason why the KC has not found widespread use in SERS. It also makes it difficult to simultaneously measure the angle-dependent reflectivity.

Conversely, we focus here on an optimization of the much-simpler backscattering configuration that does not require a special setup and is compatible with most standard Raman systems. The principle is extremely simple: it consists of using an additional lens (typically with a long focal length) to focus the incident collimated laser beam on the back-focal plane (BFP) of the microscope objective. This allows us to create an almost parallel beam on the focal plane of the sample, and therefore combine the benefits of a high angular resolution in excitation (thanks to the collimated beam) with the much improved detection efficiency of a high NA objective. A variant of this approach, where the beam is focused off-center in the BFP of a high NA objective, is commonly used in total internal reflection fluorescence (TIRF), to excite beyond the critical angle.[46] This same variant was also recently applied to SPR microscopy in ref 47.

The modified optical setup is shown schematically in Figure 4a, and it requires minimal modifications to a standard Raman system. The exact position of the additional lens (referred as the BFP) along the optical axis is not critical, and it can be adjusted experimentally by visually monitoring the beam divergence after the objective in the far-field. Care must however be taken to align the BFP lens laterally so that the excitation follows the main optical path (and is therefore matched to the axis and the collection field-of-view of the objective).

As a proof of principle, we have applied this setup to the more difficult case of gold films (which are arguably much more relevant for applications such as SPR spectroscopy). Their quality, stability, and absence of roughness can be assured with high reliability. However, the SERS signals on gold films in the KC are typically smaller than for silver for two main reasons. First, the SERS enhancement factor is predicted to be smaller at 647 nm due to the different dielectric functions of Au and Ag.[4] But perhaps more importantly, silver films are much more likely to suffer from roughness, thereby enhancing dramatically the SERS signals. This is not desirable from the point of view of SPR spectroscopy because roughness may affect the resonance quality (sharpness). It is not desirable either from the point of view of SERS, because it defeats the original purpose of uniform and controllable enhancements.

Results obtained on a gold/air interface (50 nm Au film on glass) with the layout of Figure 4a are displayed between Figures 4b and 5. We shall concentrate on the discussion of these figures for the rest of this section. Figure 4b shows the SERS intensity of the 590 cm^{-1} Raman mode of NB deposited on Au as a function of the incident (internal) angle θ for a ×10 objective with a BFP lens (50 cm focal length). As before, the solid (red) line in Figure 4b represents the parameter-free theoretical prediction which includes the effect of the numerical aperture of the collecting lens but with a collimated incident beam thanks to the BFP lens. As can be appreciated, we can now obtain the SERS spectrum with the ×10 objective, while we could hardly couple to the resonance at all (Figure 3) in the situation without the BFP lens. The data in Figure 4b is complemented by Figure 5 where we show the SERS and SPR spectra taken simultaneously for three different conditions: ×4 objective on its own, ×4 objective with BFP lens, and ×10 with BFP lens. It is clear from the data in Figure 5a that now we can benefit in collection from the higher numerical aperture of the objective, with the ×10 objective giving the best signal. From Figure 5b, on the other hand, we can appreciate how much better the coupling to the resonance is with the presence of the BFP lens. In fact, the ×4 and ×10 objectives achieve almost zero reflectivity at the

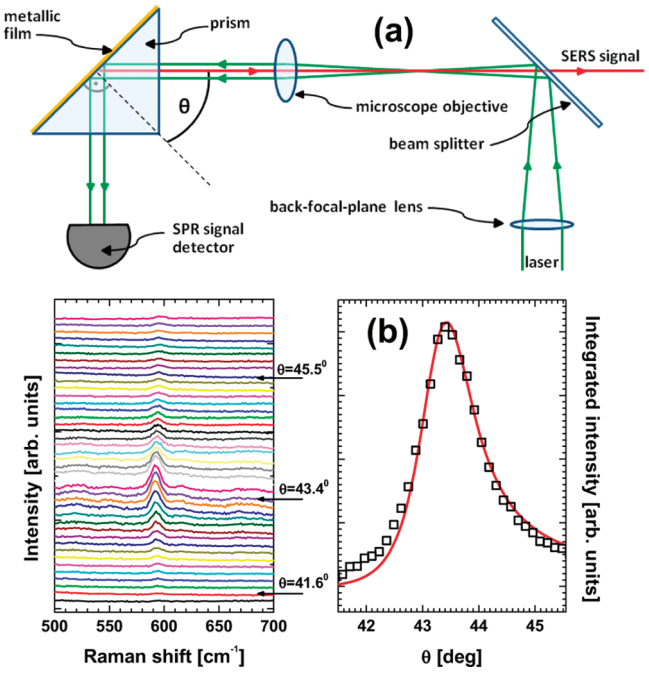

Figure 4. (a) Optical setup with BFP illumination. The first lens before the beamsplitter focuses the light on the back focal plane of the collecting lens, thus achieving a parallel beam in excitation. On the other hand, the BFP lens does not participate in the collection process, which now benefits fully from the numerical aperture of the collecting lens. This method (but with an off-axis beam) is widely used in total internal reflection fluorescence,[46] while here it is used for "on-axis" excitation. In part b we show the integrated intensity of the 590 cm^{-1} mode of NB through the resonance for a gold film (50 nm) on glass and 647 nm laser excitation (TM) using a ×10 objective and a BFP lens with 50 cm focal length. The integration time was 2 × 5 s, with laser power 2.1 mW. The data is complemented with further examples on the simultaneous performance of SERS and SPR signals for various collecting lenses in Figure 5. The solid (red) line in part b is the parameter-free theoretical prediction for the SERS intensity. See the text for further details.

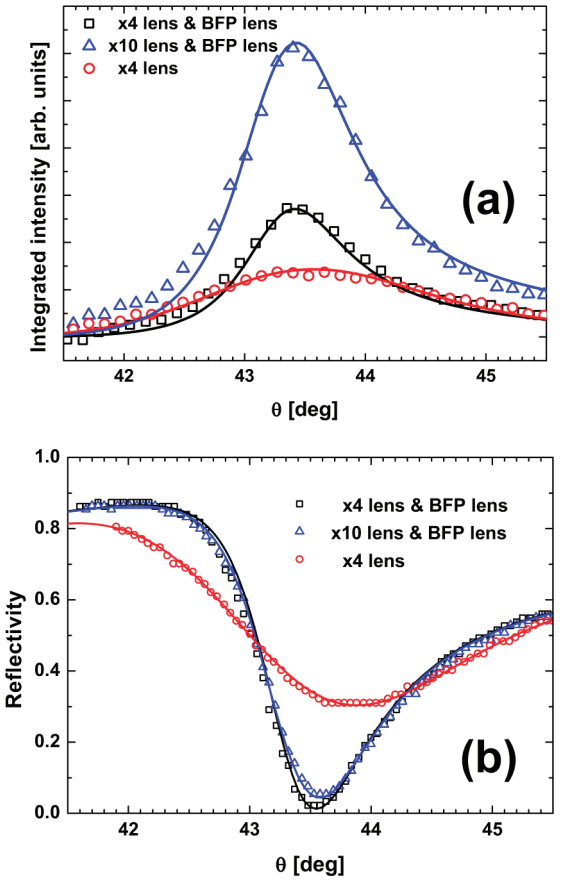

Figure 5. (a) Integrated Raman intensity of the 590 cm^{-1} mode of NB and (b) SPR (reflectivity) signal for various backscattering Kretschmann configurations at a Au/air interface (the optical setup is the same as shown in Figure 4a). The data in Figure 5b is repeated here in part a to compare it with the other cases of ×4 objective with BFP illumination and ×4 objective without it. Both the SERS signal and the SPR reflectivity data demonstrate how the coupling is improved by including the BFP lens in the case of the ×4 objective. In addition, the data shows that with the inclusion of the BPF lens the signal improves for a higher numerical aperture objective (×10 BFP with respect to ×4 BFP). Solid lines are theoretical predictions. The agreement with experiment is outstanding, thus demonstrating the potential predicting power of the technique. The integration time for the Raman spectra was 2 × 5 s, with laser power 6.4 mW (×4 with BFP), 2.1 mW (×10 with BFP), and 2.3 mW (×4).

resonance (meaning that most of the power of the laser is being funneled into SPPs on the film). This situation is very different from that of Figure 3 where the coupling was affected by the divergence of the incoming beam. The other important point to emphasize here is that all the lines in Figure 5a,b are parameter-free predictions from theory, except for a trivial scaling factor for the integrated SERS intensity (since the Raman intensity, as given by the CCD counts, depends on many factors that are purely technical, the scaling factor has no physical meaning). We judge the agreement to be outstanding. This is a point that cannot be underestimated in a technique like SERS, where exact quantification and modeling are in many cases somewhat disconnected from experimental evidence, or only connected at a qualitative level. We believe the data in Figures 4 and 5 and the quality of the agreement with theory proves beyond doubt the potential of combined SPR−SERS spectroscopy. One of the main applications of SPR in biology,[17−21] however, is done at the Au/water interface where the dynamics of binding is normally studied. Accordingly, we demonstrate in the next subsection the application of combined SPR−SERS to this specific situation.

Generalization to Au/Water Interfaces. In order to fully realize the potential of combining the commercially available SPR systems with SERS, in a dual-detection capability, it is also necessary to demonstrate its viability at the commonly used Au/water interface. This is explicitly shown in Figure 6. For these experiments we used a sapphire prism, which has a larger index of refraction (n = 1.766) and therefore is more suited to achieve the resonance condition with water (n = 1.33) at a reasonable incident angle. A liquid cell was specially designed to attach to the metal film glass slide by capillary forces. Figure 6a shows both the actual raw data for the 590 and 1650 cm^{-1} peaks of NB through the resonance, and the integrated intensity of the 590 cm^{-1} mode as a function of the internal (in glass slide) incident angle θ. Figure 6b complements the picture with the simultaneous measurement of the SPR signal. The experiment was carried out with a ×4 objecitve and shows an almost perfect coupling to the resonance in the dip of the reflectivity. As before, the solid (red) lines in Figure 6a,b are parameter-free theoretical predictions. There is a whole set of possibilities that are opened up by this result. The connection with biological applications of SPR spectroscopy already pointed out is an obvious one. But it

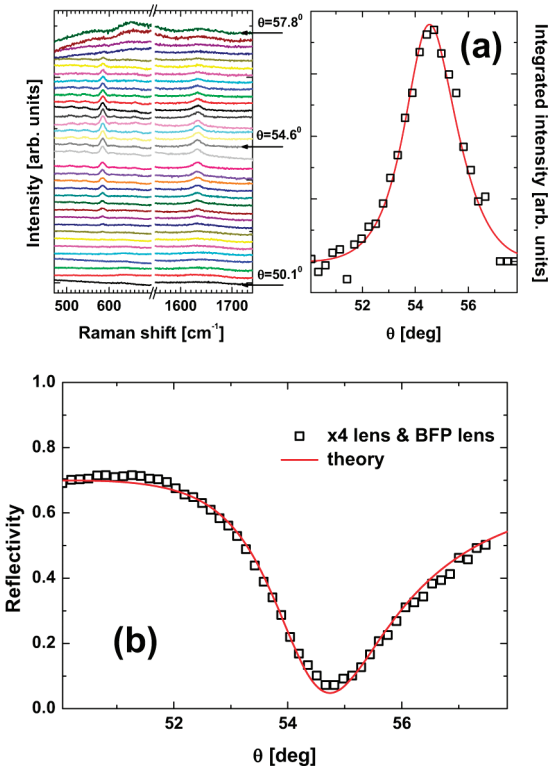

Figure 6. (a) Raw data for the 590 and 1650 cm^{-1} Raman modes of NB and integrated intensity of the 590 cm^{-1} mode across the resonance. Integration time was 2 × 2 s, with laser power 2.0 mW. These experiments were carried out on a 50 nm Au film in water at 633 nm, excitation with ×10 BFP illumination, and TM polarization. In part b we show the simultaneous measurement of the reflectivity (SPR signal) showing a high degree of coupling. The solid (red) curves in parts a and b are the theoretical predictions. For this experiment, the dye is deposited on the Au film beforehand, and then exposed to a liquid cell with water; i.e., the dye is not dissolved in solution. See the text for further details.

might also prove to be a useful tool in the study of other phenomena like surface-enhanced fluorescence.[48] If the analyte is dissolved in the liquid, the evanescent field of the SPPs penetrates a considerable distance into it. Molecules that are not directly attached to the surface do not have their fluorescence completely quenched.[4]

CONCLUSION AND OUTLOOK

For a technique that has been overlooked for potential applications in SERS for decades, we believe that the results of our paper present all the key proof-of-principle points to demonstrate that there is a promising way ahead for it. In particular, the fact that doing SERS in the Kretschmann configuration is compatible with existing spectroscopic platforms for SPR spectroscopy in liquids (and with gold substrates) opens endless possibilities. The combination of the two techniques might open new horizons in both biospectroscopy and (at a more fundamental level) the study of surface-enhanced/quenched fluorescence. Clearly the next challenge is to show the performance of the two techniques for nonresonant molecules. Besides the fact that uniform enhancements over large areas are achieved (a very desirable feature that we confirmed by doing spatial scans), the main beauty of the approach relies mainly in its predictability, in the fact that surface-plasmon-polaritons on flat surfaces represent the simplest plasmonic system and are more susceptible to predictions and quantifications[4] than standard substrates based on nanotechnology. A series of developments from here are easily envisioned to improve our control further and fulfill the potential of the technique on both fundamental and applied topics.

ASSOCIATED CONTENT

Supporting Information. Additional information as noted in text. This material is available free of charge via the Internet at http://pubs.acs.org.

ACKNOWLEDGMENT

E.C.L.R. acknowledges support from the New Zealand government and the Royal Society of New Zealand through a Marsden Grant and Rutherford Discovery Fellowship.

REFERENCES

(1) Moskovits, M. *Rev. Mod. Phys.* **1985**, *57*, 783.
(2) Dieringer, J. A.; McFarland, A. D.; Shah, N. C.; Stuart, D. A; Whitney, A. V.; Yonzon, C. R.; Young, M. A.; Zhang, X.; Duyne, R. P. V. *Faraday Discuss.* **2006**, *132*, 9.
(3) Moskovits, M. *J. Raman Spectrosc.* **2005**, *36*, 485.
(4) Le Ru, E. C.; Etchegoin, P. G. *Principles of Surface Enhanced Raman Spectroscopy and Related Plasmonic Effects*; Elsevier: Amsterdam, 2009.
(5) Aroca, R. F., *Surface-Enhanced Vibrational Spectroscopy*; John Wiley & Sons: Chichester, U.K., 2006.
(6) Smith, W. E. *Chem. Soc. Rev.* **2008**, *37*, 955.
(7) Green, M.; Liu, F. M. *J. Phys. Chem. B* **2003**, *107*, 13015.
(8) Haynes, C. L.; Duyne, R. P. V. *J. Phys. Chem. B* **2001**, *105*, 5599.
(9) Jackson, J. B.; Westcott, S. L.; Hirsch, L. R.; West, J. L.; Halas, N. J. *Appl. Phys. Lett.* **2003**, *82*, 257.
(10) Sabatte, G.; Keir, R.; Lawlor, M.; Black, M.; Graham, D.; Smith, W. *Anal. Chem.* **2008**, *80*, 2351.
(11) Noguez, C. *J. Phys. Chem. C* **2007**, *111*, 3806.
(12) McCabe, A. F.; Eliasson, C.; Prasath, R. A.; Hernandez-Santana, A.; Stevenson, L.; Apple, I.; Cormack, P. A. G.; Graham, D.; Smith, W. E.; Corish, P.; Lipscomb, S. J.; Holland, E. R.; Prince, P. D. *Faraday Discuss.* **2006**, *132*, 303.
(13) Graham, D.; McLaughlin, C.; McAnally, G.; Jones, J. C.; White, P. C.; Smith, W. E. *Chem. Commun.* **1998**, 1187.
(14) Lim, D. K.; Jeon, K. S.; Kim, H. M.; Nam, J. M.; Suh, Y. D. *Nat. Mater.* **2010**, *9*, 60.
(15) Perney, N. M. B.; Baumberg, J. J.; Zoorob, M. E.; Charlton, M. D. B.; Mahnkopf, S.; Netti, C. M. *Opt. Express* **2006**, *14*, 847.
(16) Kretschmann, E. *Z. Phys* **1971**, *241*, 313.
(17) O'Shannessy, D. J. *Curr. Opin. Biotechnol.* **1994**, *5*, 65.
(18) Malmqvist, M. *Curr. Opin. Immunol.* **1993**, *5*, 282.
(19) Szabo, A.; Stolz, L.; Granzow, R. *Curr. Opin. Struct. Biol.* **1995**, *5*, 699.
(20) Fisher, R. J.; Fivash, M. *Curr. Opin. Biotechnol.* **1994**, *5*, 389.
(21) Margulies, D. H.; Plaksin, D.; Khilko, S.; Jelonek, M. T. *Curr. Opin. Immunol.* **1996**, *8*, 262.
(22) Maier, S. A. *Plasmonics, Fundamentals and Applications*; Springer: Berlin, 2007.
(23) Novotny, L.; Hecht, B. *Principles of Nano-Optics*; Cambridge University Press: Cambridge, 2006.
(24) Otto, A. *Z. Phys.* **1968**, *216*, 398.
(25) Kretschmann, E.; Raether, H. *Z. Naturforsch., A: Astrophys., Phys. Phys. Chem.* **1968**, *23*, 2135.
(26) Moskovits, M. *J. Chem. Phys.* **1982**, *77*, 4408.
(27) Le Ru, E. C.; Meyer, M.; Blackie, E.; Etchegoin, P. G. *J. Raman Spectrosc.* **2008**, *39*, 1127.
(28) Chen, Y. J.; Chen, W. B.; Burstein, E. *Phys. Rev. Lett.* **1976**, *36*, 1207.

(29) Pettinger, B.; Tadjeddine, A.; Kolb, D. M. *Chem. Phys. Lett.* **1979**, *66*, 544.
(30) Dornhaus, R.; Benner, R. E.; Chang, R. K. *Surf. Sci.* **1980**, *101*, 367.
(31) Tom, H. W. K.; Chen, C. K.; de Castro, A. R. B.; Shen, Y. R. *Solid State Commun.* **1982**, *41*, 259.
(32) Ushioda, S.; Sasaki, Y. *Phys. Rev. B* **1983**, *27*, 1401.
(33) Corn, R. M.; Philpott, M. R. *J. Chem. Phys.* **1984**, *80*, 5245.
(34) Kurosawa, K.; Pierce, R. M.; Ushioda, S. *Phys. Rev. B* **1986**, *33*, 789.
(35) Giergiel, J.; Reed, C. E.; Hemminger, J. C. *J. Phys. Chem.* **1988**, *92*, 5357.
(36) Byahut, S.; Furtak, T. E. *Rev. Sci. Instrum.* **1990**, *61*, 27.
(37) Wittke, W.; Hatta, A.; Otto, A. *Appl. Phys. A: Solids Surf.* **1989**, *48*, 298.
(38) Futamata, M. *Langmuir* **1995**, *11*, 3894.
(39) Futamata, M.; Keim, E.; Bruckbauer, A.; Schumacher, D.; Otto, A. *Appl. Surf. Sci.* **1996**, *100/101*, 60.
(40) Futamata, M. *Appl. Opt.* **1997**, *36*, 364.
(41) Brioude, A. *J. Appl. Phys.* **2000**, *88*, 6187.
(42) Critchley, K.; Cheadle, E. M.; Zhang, H. L.; Baldwin, K. J.; Liu, Q.; Cheng, Y.; Fukushima, H.; Tamaki, T.; Batchelder, D. N.; Bushby, R. J; Evans, S. D. *J. Phys. Chem. B* **2009**, *113*, 15550.
(43) Liu, Y.; Xu, S.; Tang, B.; Wang, Y.; Zhou, J.; Zheng, X.; Zhao, B.; Xu, W. *Rev. Sci. Instrum.* **2010**, *81*, 036105.
(44) These Matlab codes are part of the SPlaC package, which can be downloaded from http://www.victoria.ac.nz/raman/book/codes.aspx.
(45) Le Ru, E. C.; Etchegoin, P. G. *Chem. Phys. Lett.* **2006**, *423*, 63.
(46) Axelrod, D. *Methods Enzymol.* **2003**, *361*, 1.
(47) Huang, B.; Yu, F.; Zare, R. N. *Anal. Chem.* **2007**, *79*, 2979.
(48) Le Ru, E. C.; Etchegoin, P. G.; Grand, J.; Felidj, N.; Aubard, J.; Levi, G. *J. Phys. Chem. C* **2007**, *111*, 16076.

Supplementary information for "Combining Surface Plasmon Resonance (SPR) spectroscopy with Surface-Enhanced Raman Scattering (SERS)"

Stefan A. Meyer, Eric C. Le Ru, and Pablo G. Etchegoin

The actual experimental setup

The prism and film are attached to a high-precision motorized rotating stage as shown in Fig. S1. The coupling between the substrate and the prism is achieved by optical oil (for microscopy). A 90° optical coupler adapts the head of the Raman microscope to direct and collect the light from the Kretschmann set up either with or without an objective on the way. The far field images of the coupling to the resonance (fringe) can be seen in reflection over a white screen from the other side of the prism. The adapted head of the microscope couples the signal detection to a triple additive/subtractive Jobin Yvon T64000 spectrometer equipped with a nitrogen cooled CCD detector (Symphony) and 600 lines/mm gratings. When using the BFP-lens, we attach the lens in the delivering optical path of the laser before the internal beamsplitter of the microscope. For Metal/Water interfaces we used a sapphire prism ($n = 1.77$), while all measurements in Metal/Air interfaces are done with a glass prism ($n = 1.5$). For the measurements on a Metal/Water interface, we designed a small cell that contains the water and can be attached to the film by capillary forces.

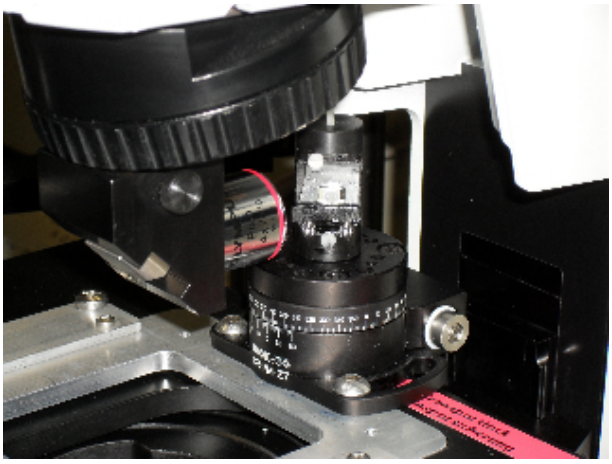

FIG. S1: Adaptation of the Raman microscope for the Kretschmann configuration.

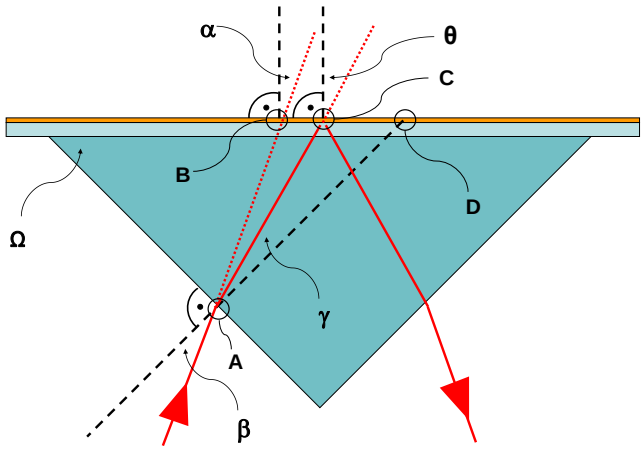

FIG. S2: Schematic illustration of a thin gold film. It shows the variables necessary to relate the internal angle of incidence θ to the external one α. If the index of refraction n_{prism} and its shape (characterized by Ω) are known, θ can be obtained from α by simple trigonometry and Snell's law.

Relating the external angle of incidence to the internal one

Experimentally, we measure for our incoming laser the angle of incidence α with respect to the normal of the sample surface (Fig. S2). However from a theoretical point of view (numerical calculation of the resonance angle etc.) we are more interested in the *internal* angle θ at the glass / metal interface (all our metal films are deposited on glass). Knowing the index of refraction of the glass-slide n_{glass}, of the prism n_{prism} and the prism's shape (characterized by the angle Ω in Fig. S2) it is possible to establish a link between α and θ.

case 1: $n_{\text{prism}} = n_{\text{glass}}$

Using Fig. S2 and Snell's law the following equations are apparent:

$$\text{ABD}: \quad \underbrace{\beta}_{\text{A}} + \underbrace{(\alpha + 90^0)}_{\text{B}} + \underbrace{(180^0 - 90^0 - \Omega)}_{\text{D}} = 180^0 \quad \text{(S1)}$$

$$\text{Snell}: \quad n_{\text{air}} \sin\beta = n_{\text{prism}} \sin\gamma \quad \text{(S2)}$$

$$\text{ACD}: \quad \underbrace{\gamma}_{\text{A}} + \underbrace{(\theta + 90^0)}_{\text{C}} + \underbrace{(180^0 - 90^0 - \Omega)}_{\text{D}} = 180^0, \quad \text{(S3)}$$

which can be rewritten as follows:

$$\text{equ.}(S1) \;\Rightarrow\; \beta = \Omega - \alpha \tag{S4}$$

$$\text{equ.}(S2) \;\Rightarrow\; \gamma = \arcsin\left(\frac{n_{\text{air}}}{n_{\text{prism}}}\sin\beta\right) \tag{S5}$$

$$\text{equ.}(S3) \;\Rightarrow\; \theta = \Omega - \gamma. \tag{S6}$$

Using Eqs. (S4) and (S5) in Eq. (S6) yields:

$$\theta = \Omega - \arcsin\left(\frac{n_{\text{air}}}{n_{\text{prism}}}\sin(\Omega - \alpha)\right) \tag{S7}$$

This last equation relates the angle α controlled with and displayed by the motorized stage to the angle of incidence θ on the metal film. Throughout the figures in the paper the x-axis for angular scans refers to this angle of incidence on the film.

case 2: $n_{\text{prism}} = n_{\text{sapphire}}$

For the case of a sapphire prism the situation is slightly more complicated: the beam is refracted not only at the air / prism interface (as in case 1) but also at the prism / glass-slide interface. At this latter interface let us call the angle of incidence $\tilde{\theta}$. Then equation (S7) is obviously still valid for $\tilde{\theta}$.

$$\tilde{\theta} = \Omega - \arcsin\left(\frac{n_{\text{air}}}{n_{\text{prism}}}\sin(\Omega - \alpha)\right) \tag{S8}$$

Once more we know from Snell's law that

$$\begin{aligned} n_{\text{prism}}\sin\tilde{\theta} &= n_{\text{glass}}\sin\theta \\ \Longrightarrow \quad \tilde{\theta} &= \arcsin\left(\frac{n_{\text{glass}}}{n_{\text{prism}}}\sin\theta\right) \end{aligned} \tag{S9}$$

Inserting now equation(S8) into equation(S9) yields

$$\begin{aligned} \theta = \arcsin\Bigg[\frac{n_{\text{pr.}}}{n_{\text{gl.}}}\sin\big(\Omega - \\ - \arcsin\left(\frac{n_{\text{air}}}{n_{\text{prism}}}\sin(\Omega - \alpha)\right)\big)\Bigg] \end{aligned} \tag{S10}$$

Sample preparation

Silver films (50 nm) were evaporated on clean glass slides using standard evaporation techniques. Gold films (50 nm nominal thickness) grown on a 2 nm Titanium adhesion layer were bought from SSens, Netherlands (with a standard RMS value of 1 nm on 1 μm for the roughness). Films were dipped in a 100 μM Nile Blue (NB) solution in water for 5 min (Ag) / 40 min (Au), and then thoroughly rinsed with water. Ultra-pure water was used for sample preparation, as otherwise impurity islands form on the films and substantially diminish the signal homogeneity. The films are cut to the appropriate size and attached to the coupling prism through an oil layer to avoid a discontinuity in the index of refraction. The homogeneity of the coverage is paramount if meaningful results are sought. We checked different preparation methods and assessed the homogeneity of the samples through Raman maps in different configurations. The surface coverage of the dye (NB) was also estimated ($\sim$ one monolayer) via electrochemical methods using the oxidation/reduction cycle of NB.

For the preparation of the liquid cell we used a procedure described in Fig. S3, with a series of pictures. From left to right: the gold sample is carefully placed on an aluminium substrate holder (picture 1) and the sapphire prism is attached to the glass side (picture 2). Now the sample is turned arround and a drop of dye-solution is placed on the gold side while a silicon o-ring is brought in place (picture 3). Finally a glass lid is placed on top and hold in place with 2 screws. This defines then a liquid layer above the metal that can be used for the studies.

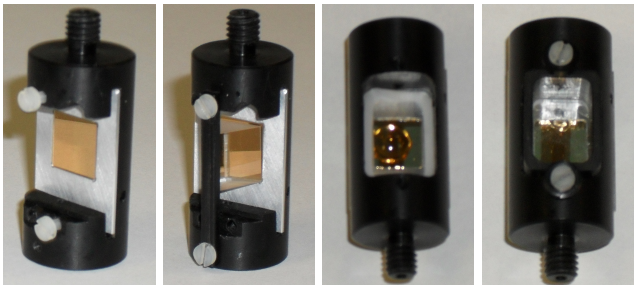

FIG. S3: Preparation of the liquid cell; from left to right: gold substrate in sample holder; sapphire prism on glass side (of gold substrate); drop of liquid on gold side of substrate; the sealed-off cell.